Electrical Power Quality and Utilisation, Journal *Vol. XI, No. 2, 2005*

Conducted EMI Mitigation in Switched Mode DC-DC Converters by Spread Spectrum Techniques

Artur KNITTER, Jarosław ŁUSZCZ, Piotr J. CHRZAN

Gdansk University of Technology, Poland

***Summary*: In this paper effectiveness of spread spectrum modulation techniques to the electromagnetic interference (EMI) suppression is investigated. Comparative evaluation of spread spectrum methods is reviewed and demonstrated with the aid of function generator and EMI receiver. Obtained results indicate advantageous features of random carrier frequency modulation (CFM), which results in more steady spectral distribution. For a switch mode dc-dc converter, random and periodical sinusoidal CFM is systematically tested. Based on disturbance voltage measurements using Line Impedance Stabilization Network (LISN) and EMI receiver, conducted emission spectra are evaluated in function of the defined randomness index *R* and frequency range. For the acceptable range of *R* variations up the 20dB EMI suppression level was reached.**

Key words:
spread spectrum, carrier frequency modulation, EMI suppression, electromagnetic compatibility

1. INTRODUCTION

Technological progress in building of semiconductor devices makes possible growth of power and frequency of switching the power electronics devices. This leads to desirable growth of voltage rise and fall rate decreasing switching losses, but also to increase of electromagnetic interference EMI emissions and acoustic noise [2]. It may be interfered other electronic equipment being in common electromagnetic environment. Acceptable EMI levels, defined in standards may be difficult to fulfilment, especially at the demanded rapid product prototyping process [13]. It exists many methods of EMI suppression of converter topologies including switched mode power supplies. It has been recently reported many approaches based on suppressing the emitted power of a given switching frequency while redistributing the energy to additional harmonics by spread spectrum methods [6,9,10,12] (Fig. 1). Thus, the interference can be decreased at its origin and at relatively low cost.

In this paper spread spectrum methods are carried out by periodical sinusoidal and random CFM. After some fundamental analytical introduction of sine frequency modulation, a systematic experimental measurements are reported in order to evaluate and compare effectiveness of EMI spectra suppression.

2. SPREAD SPECTRUM METHODS

2.1. Modulated signals properties

Frequency modulated signal can be described by formula:

$$s(t) = A_C \cos\left(2\pi f_C t + k_f \int_0^T m(t)\,dt\right) \qquad (1)$$

where A_C and f_C are the amplitude and frequency of carrier wave, $m(t)$ is modulating waveform, k_f is scaling coefficient of frequency deviation Δf at given amplitude of modulating waveform:

$$k_f = \frac{\Delta f}{A_m} \qquad (2)$$

In first case, when modulated and modulating waveforms are co-sinusoidal:

$$s(t) = A_C \cos\left[2\pi f_C t + \frac{\Delta f}{f_m}\sin(2\pi f_m t)\right] \qquad (3)$$

where modulation index:

$$\beta = \frac{\Delta f}{f_m} \qquad (4)$$

This parameter directly influences frequency modulation and spectrum of modulated signals. Relationship between bandwidth B_T of modulated signal and modulation index β known as Carson's Rule [5], can be used to estimating B_T.

$$B_T = 2(\Delta f + f_m) = 2 f_m (\beta + 1) \qquad (5)$$

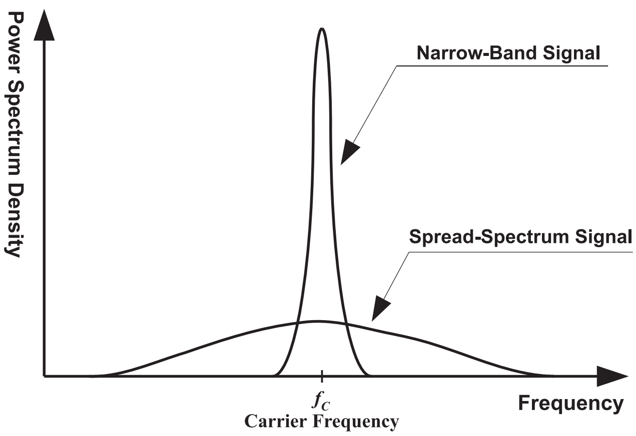

Fig. 1. Comparison of narrow-band and spread-spectrum signal envelope

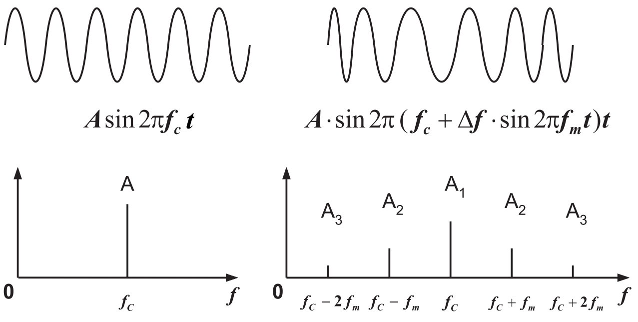

Fig. 2. Sine wave spectrum influence of carrier modulation

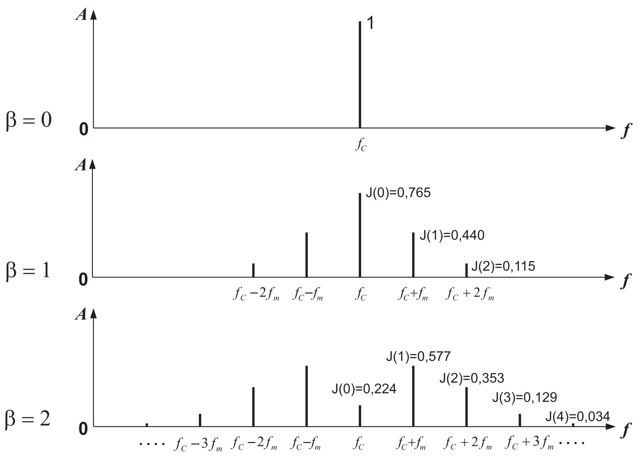

Fig. 3. Sine wave spectrum with wideband frequency modulation for modulation index β within range 0..2

Confirming this rule over 98% of total power of modulated signal is included inside bandwidth B_T [6]. From lower to upper sideband this is a range from $f_C - B_T/2$ to $f_C + B_T/2$. In several references [9], [10] randomness coefficient R has been used instead of modulation index. It is defined randomness level as difference between maximal and minimal instantaneous value normalized to the rated carrier frequency. The randomness index R is calculated as follows:

$$R = \frac{\Delta f}{f_c} \qquad (6)$$

Two types of frequency modulation (FM) can be distinguished:

– narrowband FM for $\beta << 1$;
– wideband FM for $\beta >> 1$.

At narrowband frequency modulation, modulated signal bandwidth B_T is closed to twice of modulating signal frequency f_m (5), therefore spreading of spectrum is not effective. At wideband FM each sideband is composed of a multiple harmonics, distant from carrier frequency f_C with multiple of f_m value (Fig. 2). Resulting spread spectrum is proportional to the modulation index β (5).

Amplitude of harmonics and their sidebands can be calculated on the basis of Bessel function

$$J_n(b) = \sum_{m=0}^{\infty} (-1)^m \frac{\left(\frac{b}{2}\right)^{2m+n}}{m!(m+n)!} \qquad (7)$$

where n is any integer number in interval $(-\infty, \infty)$ determining function order. Frequency modulated signal for cosine carrier and modulating function in complex form can be defined:

$$s(t) = A_C \mathrm{e}^{j\left[\Omega_C t + \frac{\Delta f}{f_m} sin(\omega_m t)\right]} = A_C \mathrm{e}^{j[\Omega_C t]} \mathrm{e}^{j[\beta\, sin(\omega_m t)]} \qquad (8)$$

where:

$\Omega_C = 2\pi f_C$ — carrier pulsation
$\omega_m = 2\pi f_m$ — modulating signal pulsation

Factor $\mathrm{e}^{j[\beta \times \sin(\omega m \times t)]}$, as periodic function with period $T_m = 2\pi/\omega_m$, can be developed as complex Fourier series of n^{th} order:

$$\mathrm{e}^{j[\beta\, sin(\omega_m \cdot t)]} = \sum_{n=-\infty}^{\infty} J_n(\beta)\, \mathrm{e}^{j\, n\omega_m t} \qquad (9)$$

Hence, from (8):

$$s(t) = A_C\, \mathrm{e}^{j(\Omega_C \cdot t)} \sum_{n=-\infty}^{\infty} J_n(\beta)\, \mathrm{e}^{j\, n\omega_m t} = $$
$$= A_C \sum_{n=-\infty}^{\infty} J_n(\beta)\, \mathrm{e}^{j(\Omega_C + n\omega_m)t} \qquad (10)$$

After conversion to real notation:

$$s(t) = A_C \begin{Bmatrix} J_0(\beta)\cos(\omega_C t) + J_1(\beta)[\cos(\omega_C - \omega_m)t + \\ +\cos(\omega_C + \omega_m)t] + J_2(\beta)[\cos(\omega_C - 2\omega_m)t + \\ +\cos(\omega_C + 2\omega_m)t] + \ldots \end{Bmatrix} \qquad (11)$$

structure spectrum of modulated signal can be depicted as in Figure 3. Resulting spread spectrum is proportional to the modulation index β.

If modulated waveform is not cosine, their spectrum is more composite (Fig. 4), for example square waveform will contain even harmonics. Frequency differences between adjacent sidebands are equal modulating frequency f_m, but for each n^{th} harmonic modulation index β_n can be express, as follows:

$$\beta_n = \frac{n\Delta f}{f_m} = n\beta \qquad (12)$$

Carson's rule is valid for each n^{th} harmonic as in equation:

$$B_{nT} = 2(n\Delta f + f_m) = 2 f_m\, (n\beta + 1) \qquad (13)$$

At wideband FM, with modulation index β growing significantly:

$$B_{nT} \underset{\beta \to \infty}{=} 2 f_m \left(n\beta \right) = nB_T \qquad (14)$$

Upper harmonics of frequency modulated signal will be more spread than lower harmonics and with possible overlapping of adjacent sidebands [6].

2.2. Spread spectrum measurements

Measurements of harmonic spectra characteristics can be obtained using digital oscilloscope, frequency analyser or EMI receiver. In first method, the signal is recorded in time domain and converted to frequency domain by fast Fourier Transform (FFT) algorithms. Accuracy of measurement is depended on sampling frequency, resolution of A/D converter and memory size [9].

Second method is based on scanning of entire frequency range of measured signal with specified velocity (dwell time Tp), frequency step and resolution bandwidth detectors (*RBW*) (Fig. 5) [7,13,14]. In EMI receivers mainly peak (P), quasi-peak (Q-P) and average value (AV) detector are available.

Output voltage of P detector responds to peak value of input voltage, therefore peak detector illustrates envelope of input signal. Using of P detector enables considerably accelerate measurements, as referred to the Q-P detector. In order to reduce measuring time, it is useful to preliminary scan with P detector the entire frequency range *"Prescan"* and next proceed to the Q-P detector for selected frequency bands *"Final Scan"*.

Response of Q-P mode detector is similar to perception of human sensual receptors. Weighted time of charge and discharge of Q-P detector have been matched in relative subjective human reaction on repeated stimuli [7,14]. Output level of Q-P detector depends on amplitude and frequency of repeated impulses given on the input, so it depends on impulse area specified as product of amplitude and duration time.

2.3. Influence of frequency modulation

In the following experimental study, the EMI receiver (Schaffner SCR3501) and the function generator (Hewlett-Packard HP33120A) have been used. All tests were made using the Q-P detector, with Tp=0,2 s and RBW=200 Hz within the 10-150 kHz scan range [14].

Firstly, the periodical carrier frequency modulation was tested for constant sinusoidal modulating frequency f_m=1kHz and variable frequency deviation Δf. The rated carrier frequency f_C=75kHz and frequency deviation Δf were assumed respectively at the 5kHz and 20kHz.

It is evident, that increasing of frequency deviation Δf (proportional increase of *b*), results in suppression of the fundamental carrier harmonic [11] (Fig. 6b). The energy of the carrier signal is spread over a wider bandwidth. In the particular measured example (Fig. 6c), sidebands of the second carrier harmonic (f_{C2}=150kHz) above 100kHz are

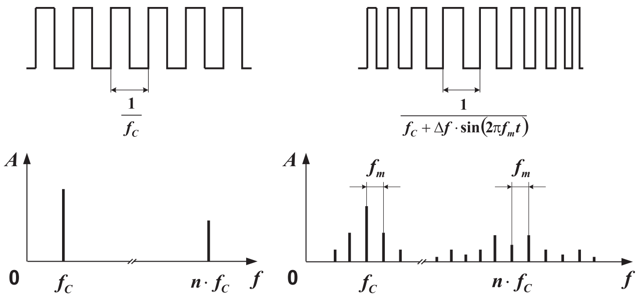

Fig. 4. Square wave spectrum without modulation and with wideband frequency modulation

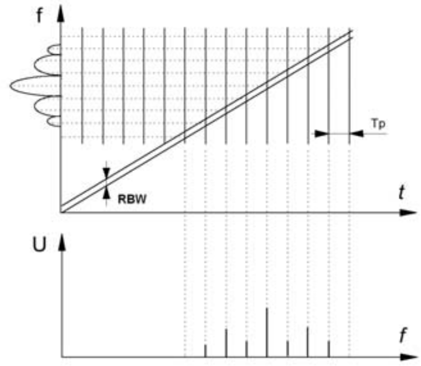

Fig. 5. Scan processing principles of the EMI receiver

distinguished, because envelope of the 2nd harmonic sidebands is twice wider than that of the fundamental carrier frequency [2,12]. However, growing index β generates distributed sidebands harmonics with increased amplitudes, as compared to no modulation case (Fig.6a). This effect may have negative consequences due to low-frequency distortion harmonics concentrated around fundamental carrier sidebands.

The second experiment deals with sinusoidal modulating frequency f_m variations at constant Δf reference. In order to investigate an influence of the Q-P detector operation, the two cases of f_m <*RBW* and f_m >*RBW* have been tested. Obtained spectra depend on the resolution bandwidth of the EMI receiver, at the case of f_m <*RBW* side band harmonics are indistinguishable, as was previously mentioned in [6] (Fig.7a). Increasing modulating frequency f_m >*RBW* results in augmented bandwidth with the overlapping effect of sidebands carrier harmonics (Fig.7b). Side-band harmonics are distributed with f_m resolution.

The following tests were carried out by the function generator at random (white noise) modulation of the carrier frequency f_C within preset frequency deviation $\pm\Delta f$ range. Increasing deviation dithering results in more effective suppression of fundamental with dispersing of harmonics around the carrier frequency (Fig. 8).

3. EXPERIMENTAL VALIDATION

An experimental switch mode dc-dc converter is based on the MOSFET transistor T (Fig. 9). The EMI receiver with the line impedance stabilization network are used for spectral measurements of the conducted disturbance level (Fig. 11).

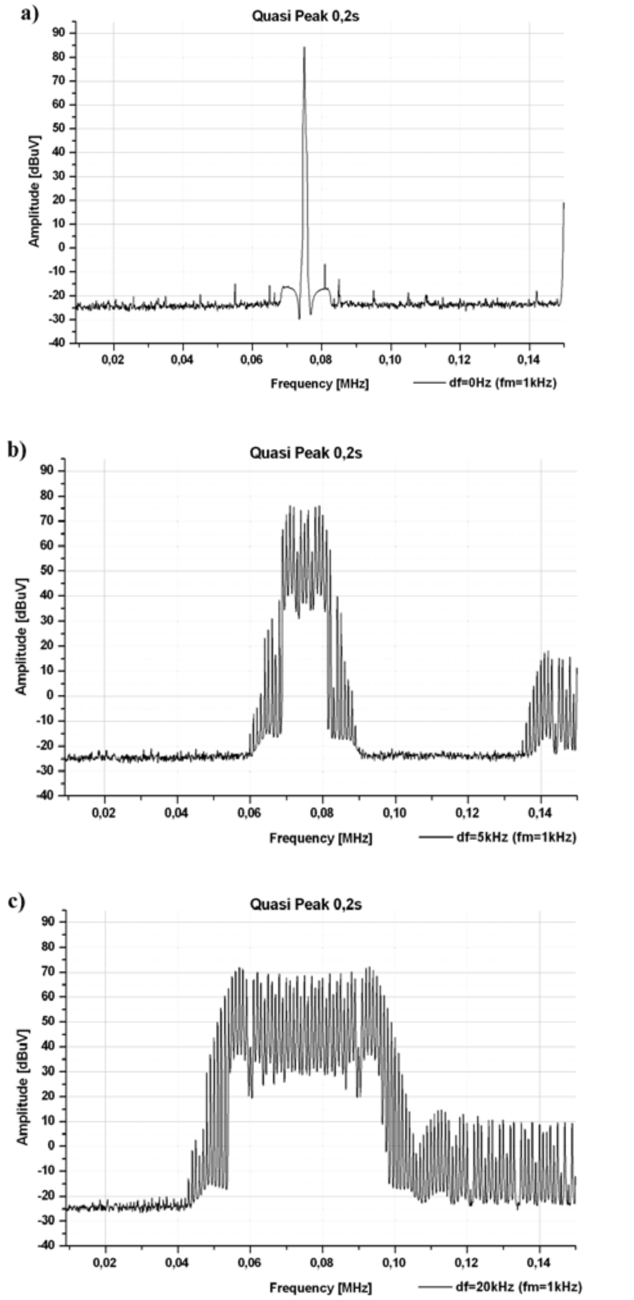

Fig. 6. Harmonic spectra at the carrier sine modulation; f_m =1kHz, Δf= a) 0Hz, b) 5kHz, c) 20kHz

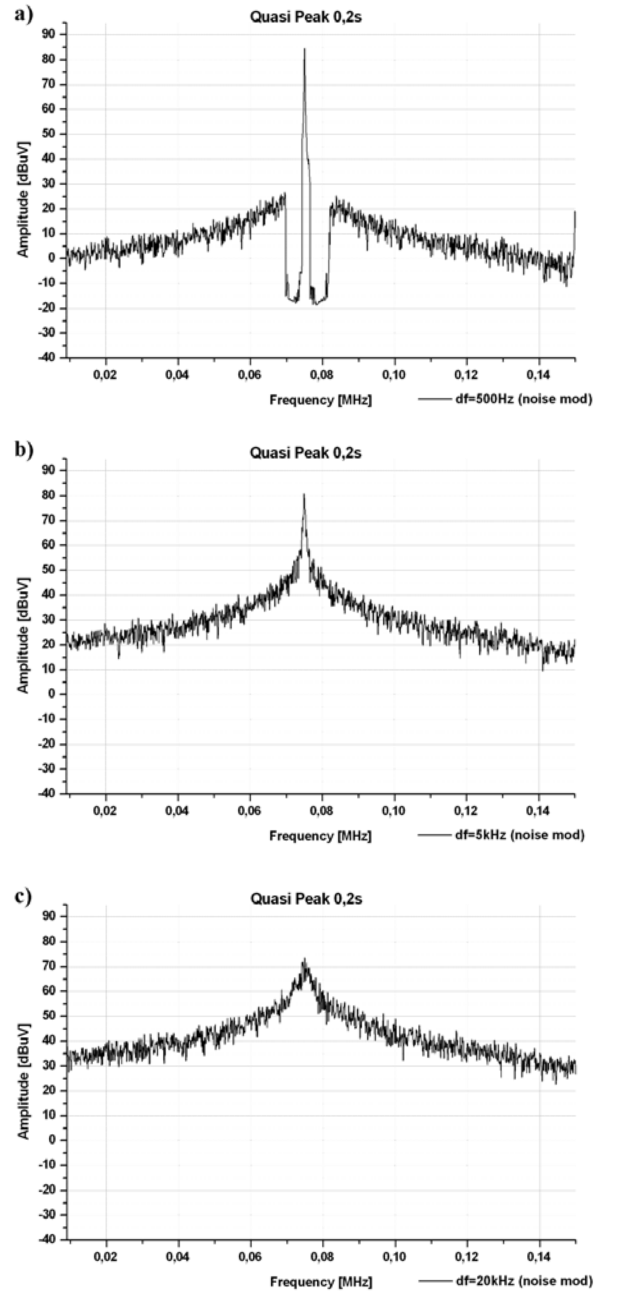

Fig. 8. Harmonic spectra at random CFM; Δf_C= a) 500Hz, b) 5kHz, c) 20kHz

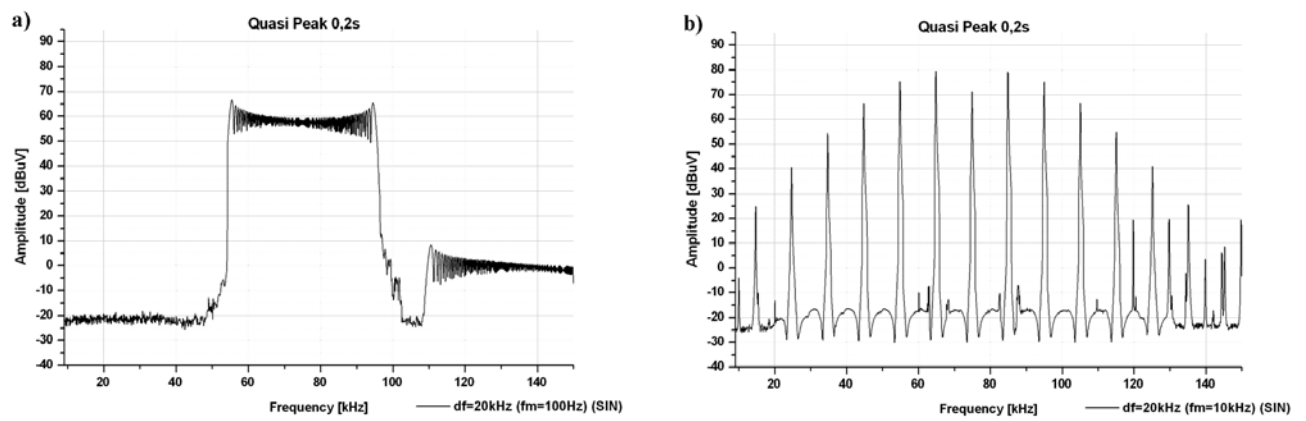

Fig. 7. Harmonic spectra at carrier sine modulation; Δf = 20kHz, f_m= a) 100Hz, b) 10kHz

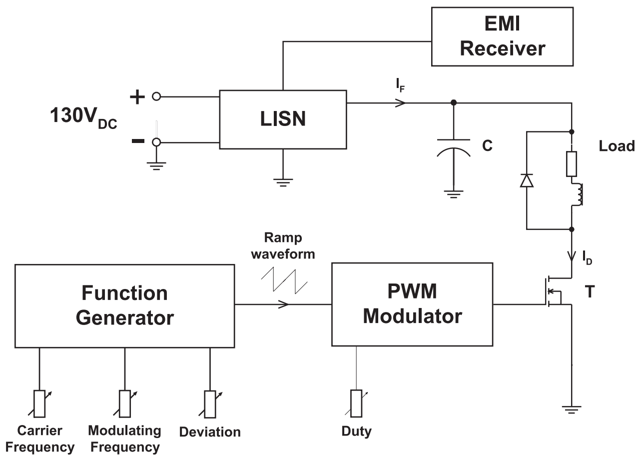

Fig. 9. Scheme of experimental setup

Converter is tested at constant reference of the duty ratio (0,5). Rated carrier frequency of ramp waveform is set at f_C=75kHz. In order to implement random and periodical sinusoidal CFM with variable frequency deviation ±Δ*f*, the function generator has been applied (Fig.10).

For higher modulation depth the ripples of load current has been observed (Fig.12). This effect limits useful range of frequency deviation Δ*f* to about 15kHz (*R*<0,2). Then ripples of load current not exceed 10% of average current value. At random CFM scheme current ripples were less harmful.

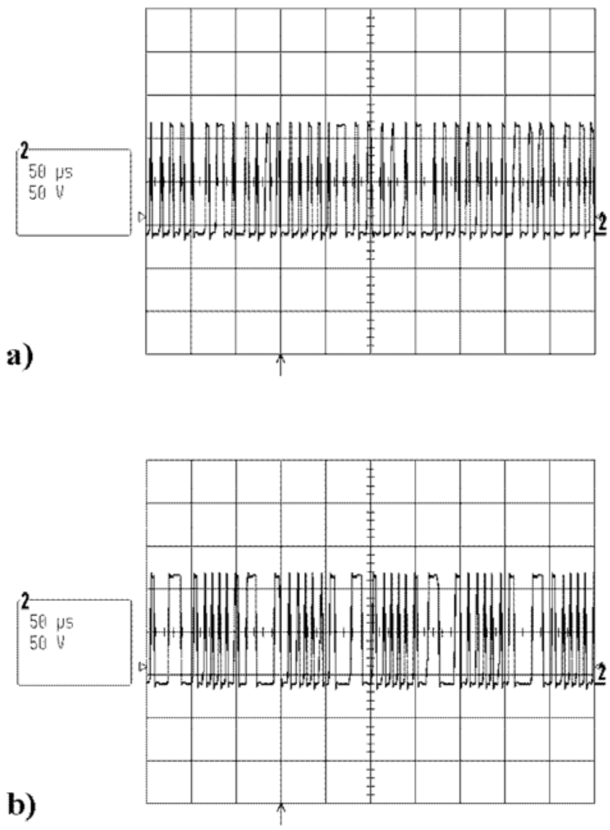

Fig. 10. Transistor U_{DS} voltage waveforms; a) random modulation, b) 10 kHz sine modulation

4. CONCLUSION

Application of carrier frequency modulation to switched mode dc-dc converters can decrease conducted EMI level and spread its emission spectrum. Systematic experimental study with the aid of EMI receiver has indicated the adequacy of quasi-peak detector to characterize the spread spectrum techniques. Comparative measurements prove advantages of random CFM than periodical sinusoidal CFM modulation in more steady spectral distribution in low frequency range and higher EMI suppression in high frequency range.

Effective mitigation of EMI depended on randomness index and modulating frequency. For *R*>0,06 carrier amplitude reduction was 5 dB, in a frequency range above 2 MHz suppression level has increased to about 18 dB. Further increase of *R* enabled suppression of fundamental carrier harmonic to 11 dB at $R = 0.2$, while obtaining only less improvement in the high frequency range. For higher values of frequency deviation Δ*f*, the ripples of load current has been developed. This limited acceptable range of randomness index to the $R < 0.2$. Frequency of ripples depended on modulating frequency or modulating waveform.

REFERENCES

1. Bech M.M., Blaabjerg F., Pedersen J.K.: *Random modulation techniques with fixed switching frequency for three-phase power converters.* IEEE Transactions on Power Electronics, 2000, 15, pp. 753–761.
2. Chrzan P.J., Haras A., Roye D.: *Random and programmed modulation schemes for power converters—microcontroller implementation,"* Int. Conf. on Power Electronics, Motion Control PEMC'94 Warszawa, 1994, I, pp. 93–98.
3. Dixon R.C.: *Spread Spectrum Systems.* John Wiley & Sons 1976.
4. Dixon R.C.: *Spread Spectrum Techniques.* John Wiley & Sons 1976.
5. Habetler T., Divan D.: *Acoustic Noise Reduction in Sinusoidal PWM Drives Using a Randomly Modulated Carrier.* IEEE Transactions on Power Electronics, 1991, 6, 3, pp. 356–363.
6. Lin F., Chen D.: *Reduction of Power Supply EMI Emission by Switching Frequency Modulation.* IEEE Transactions on Power Electronics, 1994, 9, 1, pp. 132–137.
7. Ramesh A.A., Mahesh G., Das K.: *Importance of Receiver Dwell Time in Emission Measurements.* Electromagnetic Compatibility Journal, 2000, 13, 1 & 2, pp. 33–35.
8. Ristau D., Hansen D.: *Modulation Impact On Quasi-peak Detector Response.* IEEE Int. Symp. on Electromagnetic Compatibility 1997.
9. Tse K., Shu-Hung Chung H., (Ron) Hui S., So H.: *Analysis and Spectral Characteristics of a Spread – Spectrum Technique for Conducted EMI Suppression.* IEEE Transactions on Power Electronics, 2000, 15, 2, pp. 399–410.
10. Tse K., Shu-Hung Chung H., (Ron) Hui S., So H.: *A Comparative Investigation on the Use of Random Modulation Schemes for DC/DC Converters.* IEEE Transactions on Industrial Electronics, 2000, 47, 2, pp. 253–263.
11. Tse K., Shu-Hung Chung H., (Ron) Hui S., So H.: *A Comparative Study of Carrier-Frequency Modulation Techniques for Conducted EMI Suppression in PWM Converters.* IEEE Trans. on Ind. Electronics, 2002, 49, 3, pp. 618–627.
12. Vilathgamuwa M., Deng J., Tseng K.J.: *EMI suppression with switching frequency modulated dc-dc converters.* IEEE Ind. Applications Magazine, 1999, 5, 6, pp. 27–33.
13. Władziński W.: *Influence of selected components of power electronic converter on conducted disturbances generation.* (in polish) PhD thesis from the Gdansk University of Technology 2002.
14. CISPR 16-1 *Specifications for radio disturbance and immunity measuring apparatus and methods. Part 1: Radio disturbance and immunity measuring apparatus*. 1993.

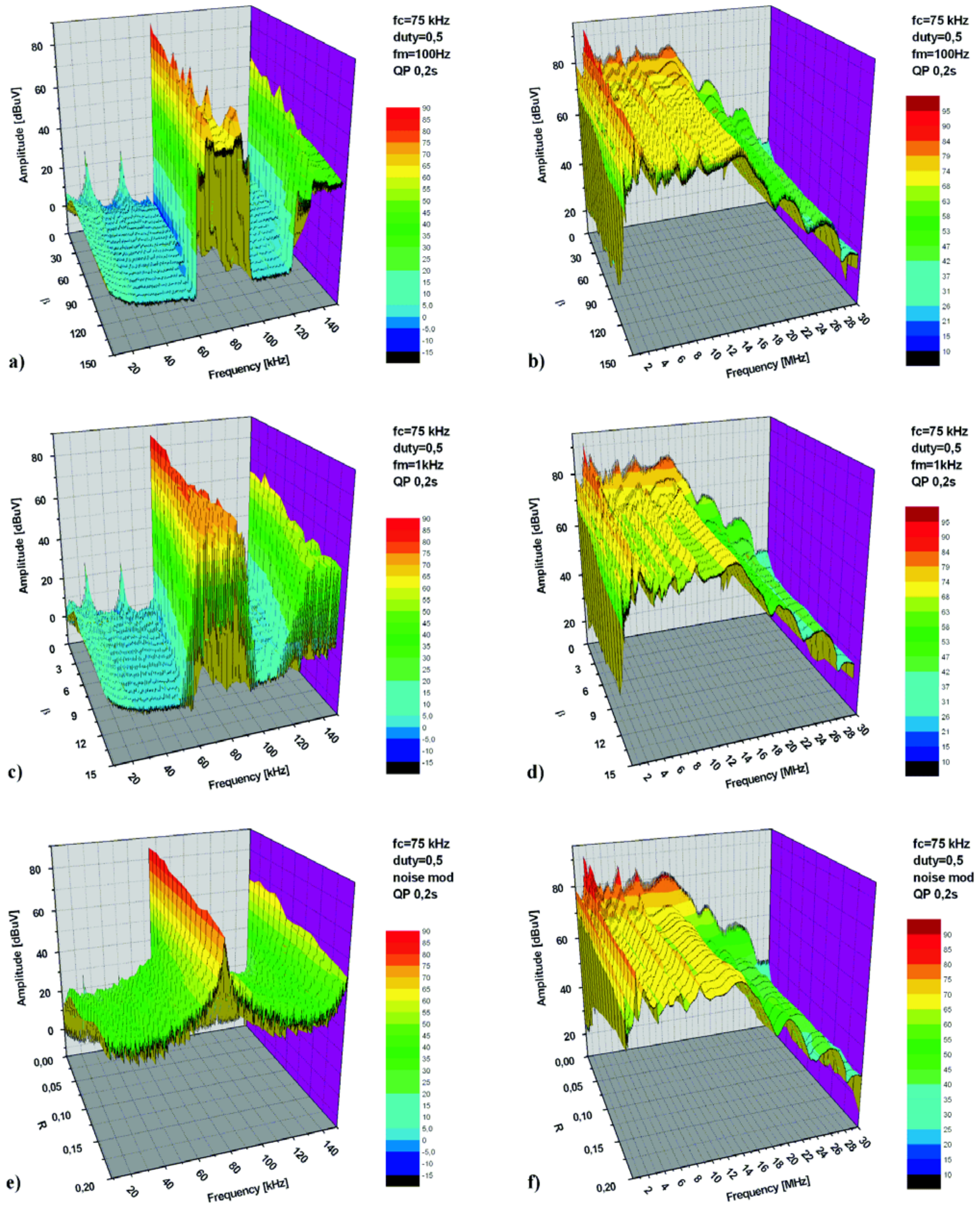

Fig. 11. Experimental spectra of conducted EMI;
a) f_m = 100 Hz: range 9–150 kHz
b) f_m = 100 Hz: range 0.15–30 MHz
c) f_m = 1 kHz: range 9–150 kHz
d) f_m = 1 kHz: range 0.15–30 MHz
e) random CFM: range 9–150 kHz
f) random CFM: range 0.15–30 MHz

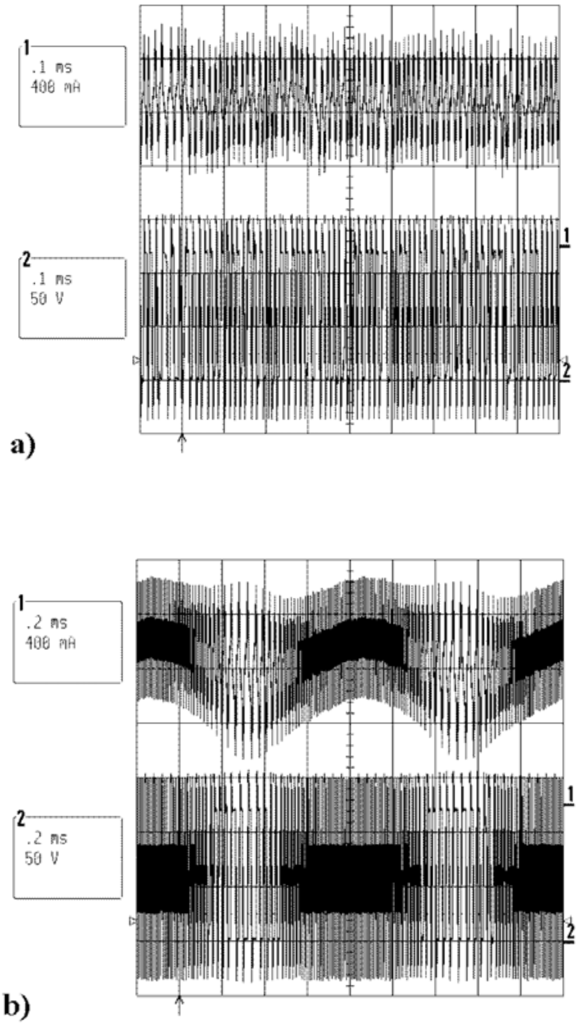

Fig. 12. Load current ripples and transistor U_{DS} voltage waveforms; a) random CFM (Df = 50kHz); b) periodical sinusoidal CFM (f_m = 1kHz; Df = 50kHz)

Artur Knitter
was born in Elbląg, Poland in 1977. He received BSc. and MSc. degrees in electrical drive and power electronics from Gdansk University of Technology in 2002 and 2003, respectively. He is currently PhD student in the Department of Electrical and Control Engineering. He is involved in projects related to EMI emission modelling in quasi-resonant power converters. His research interests include electromagnetic compatibility, energy conversion and electrical power quality.
Address:
Gdansk University of Technology
ul. G. Narutowicza 11/12, 80-952 Gdańsk, Poland
e-mail: aknitter@ely.pg.gda.pl

Jarosław Łuszcz
received the M.Sc. and PhD degrees in electrical engineering from the Gdansk University of Technology (GUT), Poland, in 1988 and 1998 respectively. Since 1999 he is an Associate Professor with the Electrical and Control Engineering Faculty at GUT. His main research interests are focused on electromagnetic compatibility applied to power electronics converters feeding AC motors drives and electromagnetic interference measurement and modelling of power electronics systems.
Address:
Gdansk University of Technology
ul. G. Narutowicza 11/12, 80-952 Gdańsk, Poland
email: jlusz@ely.pg.gda.pl

Piotr J. Chrzan
received the M.Sc., Ph.D., and Dr.Sc. degrees in 1978, 1988, and 1999, respectively, all from the Gdańsk University of Technology. Since 1980, he has been with the Faculty of Electrical and Control Engineering of the Gdańsk University of Technology. He is currently the Head of the Chair of Power Electronics and Electrical Machines. His research interests include modelling and control of electrical drives and power converters EMI optimisation. He is a member of the Editorial Committee of the Revue Internationale de Génie Electrique (Hermes-Lavoisier).
Address:
Gdansk University of Technology
ul. G. Narutowicza 11/12, 80-952 Gdańsk, Poland
e-mail: pchrzan@ely.pg.gda.pl